# Rac1 functions downstream of miR-142 in regulation of erythropoiesis

*Natalia Rivkin,[1] Elik Chapnik,[1] Yehudit Birger,[2] Eran Yanowski,[1] Caterina Curato,[3] Alexander Mildner,[3] Ziv Porat,[4] Gail Amir,[5] Shai Izraeli,[2,6] Steffen Jung[3] and Eran Hornstein[1]*

*[1]Department of Molecular Genetics, Weizmann Institute of Science, Rehovot; [2]Functional Genomics and Leukemic Research, Cancer Research Center, Sheba Medical Center, Ramat Gan; [3]Department of Immunology Weizmann Institute of Science, Rehovot; [4]Life Sciences Core Facilities, Weizmann Institute of Science, Rehovot; [5]Department of Pathology, Hadassah Medical Center, Jerusalem and [6]Department of Human Molecular Genetics and Biochemistry, Tel Aviv University, Israel*

*Correspondence: eran.hornstein@weizmann.ac.il*
*doi:10.3324/haematol.2017.171736*

**Rac1 functions downstream of miR-142 in regulation of erythropoiesis**

**Rivkin et al.**

**Online supplementary materials**

## Materials and methods

### Mouse genetics, surgical procedures and husbandry

Mouse genetics and experimentation protocols were approved by the Institutional Animal Care and Use Committee of WIS. Genotyping performed by PCR analysis of genomic tail DNA, following Chapnik *et al.* [1].

Surgical splenectomy was performed on anesthetized mice (Ketamine / Xylazine), via lateral resection under sterile conditions. After splenectomy the animals quickly recovered, gained weight and behaved normally, like age-matched control mice. Complete blood count was performed 6 to 7 weeks after splenectomy.

Injection of carrier alone (sterile PBS) or NSC23766 (2.5 mg /kg / day for 10 days; SML0952 Sigma-Aldrich) [4] was performed via intraperitoneal route.

Tissue and cellular analysis was performed 10 days after initiating administration of NSC23766.

### Hematology and histology

Whole blood at a volume of 100 µl was drawn via retro-orbital approach into glass capillary tubes that were pre-treated with 5 µl of 0.5M EDTA. A complete blood count was performed on ADVIA 120 Hematology System (Siemens Healthcare, Erlangen, Germany) by American Medical Laboratories (Herzliya, Israel). Spleens and long axial bones were dissected post euthanasia and fixed overnight in 4% paraformaldehyde. Specimens were dehydrated in graded

ethanols, washed and processed into paraffin blocks. Femora were further decalcified in 14% EDTA for 2–5 days. Longitudinal paraffin sections were stained with hematoxylin and eosin (H&E) or Reticulin staining. Bright-field micrographs captured with Olympus BX51 microscope at 40X magnification.

**Colony-forming unit assays**

Fetal liver (FL) from embryonic days 13.5-14.5 (E13.5-14.5) was dissected to single cells and $10^4$ cells were cultured in M3434 MethoCult (StemCell Technologies) with erythropoietin ( 10 U / ml), stem cell factor (50 ng / mL), IL3 (10 ng / ml) and IL6 (10 ng / ml). For BM and spleen cells the cells were plated at a density of 2 x $10^4$ and $10^5$ cells respectively per ml. When mentioned, Rac1 inhibitor, NSC23766, was added at concentrations of 5 µM or 20 µM. Erythroid colony-forming units (CFUe) from FL were enumerated after 5 days of culture and from BM and spleen after 3 days before and after benzydine staining The cultures were stained with benzidine (3% acetic acid containing 0.4% benzidine and 0.3% H2O2) to indicate the amount of erythroid colonies.

**Flow cytometry, FACS and ImageStreamX analysis**

For cell-surface erythroid cell phenotyping, freshly obtained BM, splenocytes or FL cells washed with cold PBS and stained with PE-conjugated anti-CD71 antibody (Abcam, Cambridge, England), FITC conjugated anti-Ter119 (Emfret), and Hoechst. Flow cytometric analysis was performed with an LSRII flow cytometer (BD Biosciences) and FlowJo Version 8.8.7 software (TreeStar). For cell isolation erythrocytes were sorted with antibodies against Ter119PE, and CD71FITC (eBioscience, San Diego, CA) on a Fusion Aria - BD Bioscence sorter. For

distribution of cytoskeletal molecules within enucleating BM erythroblasts, cells were collected and processed for ImageStreamX analysis as previously described [5]. Approximately 100,000 cells were analyzed with Image Data Exploration and Analysis software (IDEAS; Amnis corp., part of EMD millipore) per experimental repeat. Enucleating events were quantified using the Delta Centroid XY feature, which measures the distance (in microns) between the geometric center of two images, and can be intensity-weighted. Enucleating cells will have a higher distance between the Ter119 and Hoechst staining, but not between the Ter119 and Actin staining.

**Western blotting**

Whole-cell protein lysates were prepared from wild-type or miR-142-/- BM. 50 µg of protein lysate was separated by SDS polyacrylamide gel electrophoresis, electrotransferred onto 0.2mm nitrocellulose membrane, blocked in TBS, 0.1% Tween20 and 5% dry milk for 1h and incubated overnight with anti-Rac1 (ab155938; Abcam, 1:1,000) and anti- GAPDH (AM4300; Ambion, 1:10,000). After staining with Horseradish peroxidase-conjugated secondary antibodies (Jackson ImmunoResearch Laboratories 1:10,000) immunoreactivity was detected with enhanced chemiluminescence (GE Healthcare) captured with ImageQuant LAS4010 (GE Healthcare Life Sciences) and quantified with ImageJ [6].

**Next Generation Sequencing and quantitative real time PCR**

Total RNA was isolated with miRNeasy micro kit (Qiagen), and RNA quality was assessed with ND–1000 Nanodrop (Peqlab). For transcriptomics, 3' end next generation sequencing protocol

was performed on Illumina 2500 sequencer with 50 bp single read following [7]. Computational trimming of Illumina adaptors, 5' GGG, polyA or polyT and mapping to the mouse mm10 genome, was done with STAR v2.3.0e [8] at gene-specific windows of 500 bp upstream and 100 bp downstream of the 3' end of the last exon, maintaining a margin of at least 50 bp between nearby genes. Counting with HTSeq-count [9] and differential expression analysis with DESeq2[10]. Raw P values were adjusted for multiple testing using the procedure of Benjamini and Hochberg. miR-142 targets were predicted by TargetScan 7.1 [11]

For RT-PCR CD71-Ter+ erythrocytes were sorted from splenocytes, bone marrow or fetal liver (E13.5 ) suspensions with antibodies against Ter119PE, and CD71FITC (eBioscience, San Diego, CA) on a Fusion Aria - BD Bioscence sorter. Total RNA from sorted cells was extracted using RNAeasy micro kit (Qiagen, Valencia, CA).

Quantitative Real-time PCR (qPCR) was as in [1] with the following primers:

Cfl2 (F:TCTCGTCCCAGTGCCACCG, R:ACTCCAGATGCCATAGTGCCCGC);

Rac1 (F:TACCCGCAGACAGACGTGTT, R:GTGGTGTCGCACTTCAGGAT);

Hprt (F:CTGGTTAAGCAGTACAGCCCCAAA, R:TGGCCTGTATCCAACACTTCGAGA);

Gata1 (F:TCACAAGATGAATGGTCAGA, R:TGGTCGTTTGACAGTTAGTG);

Gata2 (F:CACCCCTATCCCGTGAATCC, R:GGCGGCCACTCGCAG);

Klf1 (F:CCTCCATCAGTACACTCACC, R:CCTCCGATTTCAGACTCACG);

Tal1 (F:GTTTCGCCTATTTCTGACCGC, R:TTAGGACCTCCACTCCTCCG);

Ldb1 (F:CTTAGTCCTCACCCTTGCCA, R: GCTTGAATGACTTTGAGGAACA);

Lmo2 (F:ATCGAAAGGAAGAGCCTGGA, R: TAGCGGTCCCCTATGTTCTG);

Alas2 (F:CAGGGCAACAGGACTTTGGG, R:GGGGCAGCGTCCAATACTAA);

Fech (F:GACCCCTATCCCCAAGAGGT, R: ACTGGACCAACCTTGGACTG);

Epor (F: AGGGCTGCATCATGGACAAA, R: CAGGGCCGCTTTGCTCT);

Hbb (F:GCTTCTGACATAGTTGTGTTG, R:CTGAAGTTCTCAGGATCCACA);

Hba (F: ATGTTTGCTAGCTTCCCCACCACCAAG, R: GGTGGCTAGCCAAGGTCACCAGCA);

Hb-y (F: TGGCCTGTGGAGTAAGGTCAA, R: GAAGCAGAGGACAAGTTCCCA);

Hb-bh (F: TGGACAACCTCAAGGAGACC, R: ACCTCTGGGGTGAATTCCTT);

mDia2 (F:AAGCTTCTGTCTGCAGTGTGCA, R: GAGGCCTTCCACAATGGAAAA);

Rac2 (F: GTGGCGTTCTTTCCCAGTTA, R: CGAGAGAGGTGTCAGGAAGG);

miR-142-3p (F:TGTAGTGTTTCCTACTTTATGGA, R: universal)

miR-142-5p (F:CATAAAGTAGAAAGCACTACT, R: universal)

RNU6B (U6) (F:GATGACACGCAAATTCGTGAA, R: universal)

**Statistical analyses**

Expression values of all human mRNAs at several stages of erythropoiesis were obtained from next generation sequencing data in supplemental table 3 of [12]. miR-142-3p.1 target genes are from Targetscan 7.1 (human) [11]. cumulative distribution fraction (CDF ) was calculated using GraphPad Prism on reads per Kilobase of transcript per Million mapped reads (RPKM). For graphic purpose, Log2-RPKM values were standardized.

**References for Supplementary material of Rivkin et al.,**

1. Chapnik E, Rivkin N, Mildner A, Beck G, Pasvolsky R, Metzl-Raz E, et al. miR-142 orchestrates a network of actin cytoskeleton regulators during megakaryopoiesis. Elife. 2014;3:e01964.
2. Vemula S, Shi J, Mali RS, Ma P, Liu Y, Hanneman P, et al. ROCK1 functions as a critical regulator of stress erythropoiesis and survival by regulating p53. Blood. 2012 Oct 4;120(14):2868-78.

3. Gutierrez L, Tsukamoto S, Suzuki M, Yamamoto-Mukai H, Yamamoto M, Philipsen S, et al. Ablation of Gata1 in adult mice results in aplastic crisis, revealing its essential role in steady-state and stress erythropoiesis. Blood. 2008 Apr 15;111(8):4375-85.
4. Yuzugullu H, Baitsch L, Von T, Steiner A, Tong H, Ni J, et al. A PI3K p110beta-Rac signalling loop mediates Pten-loss-induced perturbation of haematopoiesis and leukaemogenesis. Nat Commun. 2015 Oct 07;6:8501.
5. Konstantinidis DG, Pushkaran S, Johnson JF, Cancelas JA, Manganaris S, Harris CE, et al. Signaling and cytoskeletal requirements in erythroblast enucleation. Blood. 2012 Jun 21;119(25):6118-27.
6. Schindelin J, Rueden CT, Hiner MC, Eliceiri KW. The ImageJ ecosystem: An open platform for biomedical image analysis. Mol Reprod Dev. 2015 Jul-Aug;82(7-8):518-29.
7. Lavin Y, Winter D, Blecher-Gonen R, David E, Keren-Shaul H, Merad M, et al. Tissue-resident macrophage enhancer landscapes are shaped by the local microenvironment. Cell. 2014 Dec 4;159(6):1312-26.
8. Dobin A, Davis CA, Schlesinger F, Drenkow J, Zaleski C, Jha S, et al. STAR: ultrafast universal RNA-seq aligner. Bioinformatics. 2013 Jan 1;29(1):15-21.
9. Anders S, Pyl PT, Huber W. HTSeq-a Python framework to work with high-throughput sequencing data. Bioinformatics. 2015 Jan 15;31(2):166-9.
10. Love MI, Huber W, Anders S. Moderated estimation of fold change and dispersion for RNA-seq data with DESeq2. Genome Biol. 2014 Dec 5;15(12):550.
11. Agarwal V, Bell GW, Nam JW, Bartel DP. Predicting effective microRNA target sites in mammalian mRNAs. Elife. 2015;4.
12. An X, Schulz VP, Li J, Wu K, Liu J, Xue F, et al. Global transcriptome analyses of human and murine terminal erythroid differentiation. Blood. 2014 May 29;123(22):3466-77.

**Supplementary Figures**

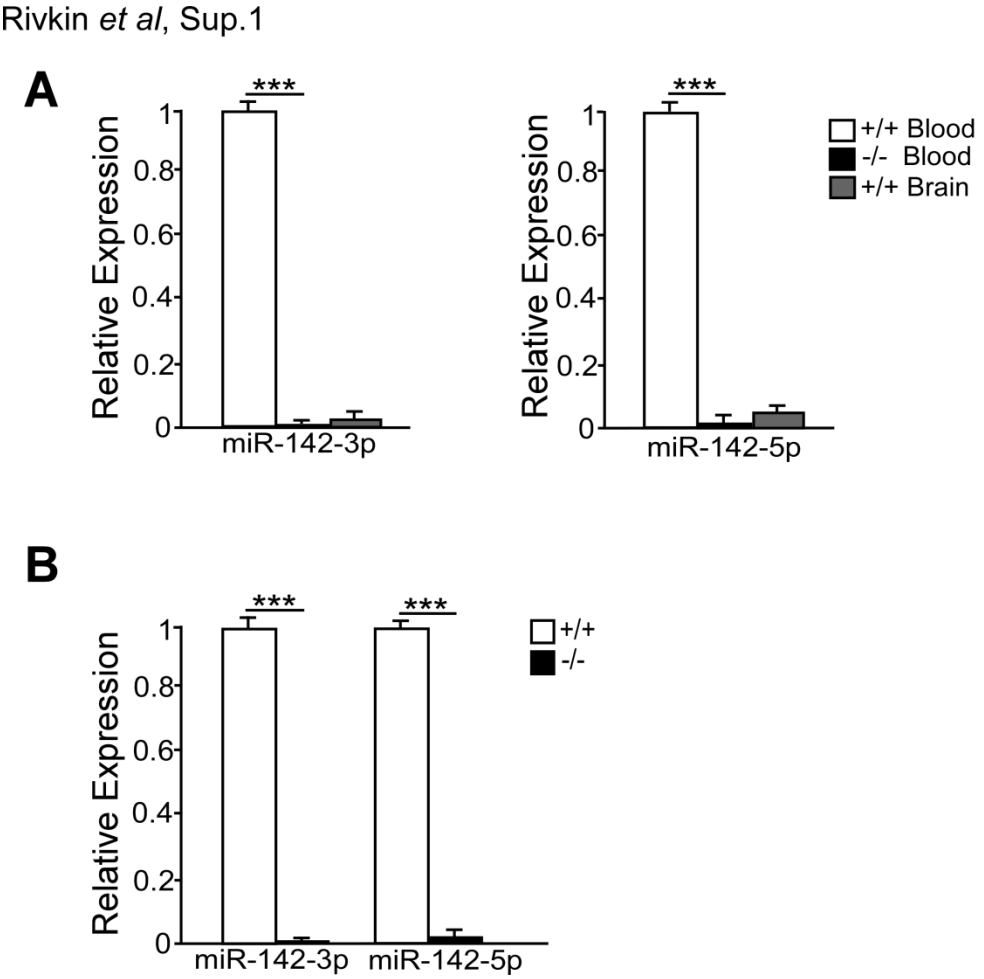


**Sup. Figure 1: Expression levels of miR-142 in blood and brain of the miR-142-/- allele. (A)** Quantitative real-time (qPCR) performed on cDNA from blood and brain, reveal nullification of miR-142-3p and miR-142-5p expression in miR-142−/− animals relative to controls (n=3 mice, per group). **(B)** Quantitative real-time (qPCR) performed on cDNA from red blood cells, reveal nullification of miR-142-3p and miR-142-5p expression in miR-142−/− animals relative to controls (n=3 mice, per group). Two tailed student t-test, Error bars, mean ±SEM, *** P<0.001 ns

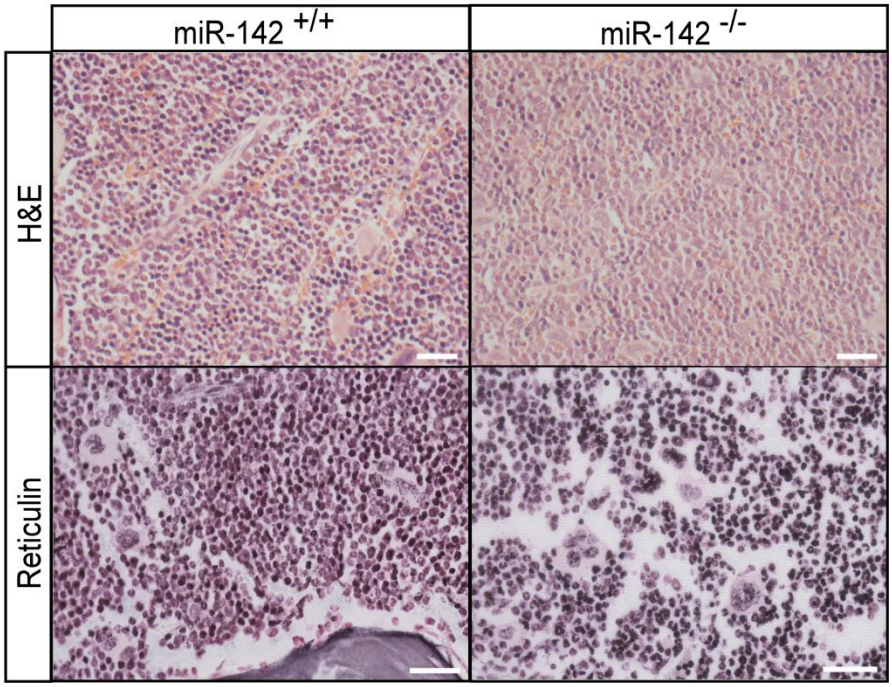


**Sup. Fig. 2: The bone marrow of miR-142-/- animals is not fibrotic.** Hematoxylin and Eosin (H&E, upper), or Reticulin (lower) staining of femur sections. Scale bars, 100 μm.

Rivkin *et al*, Sup.3

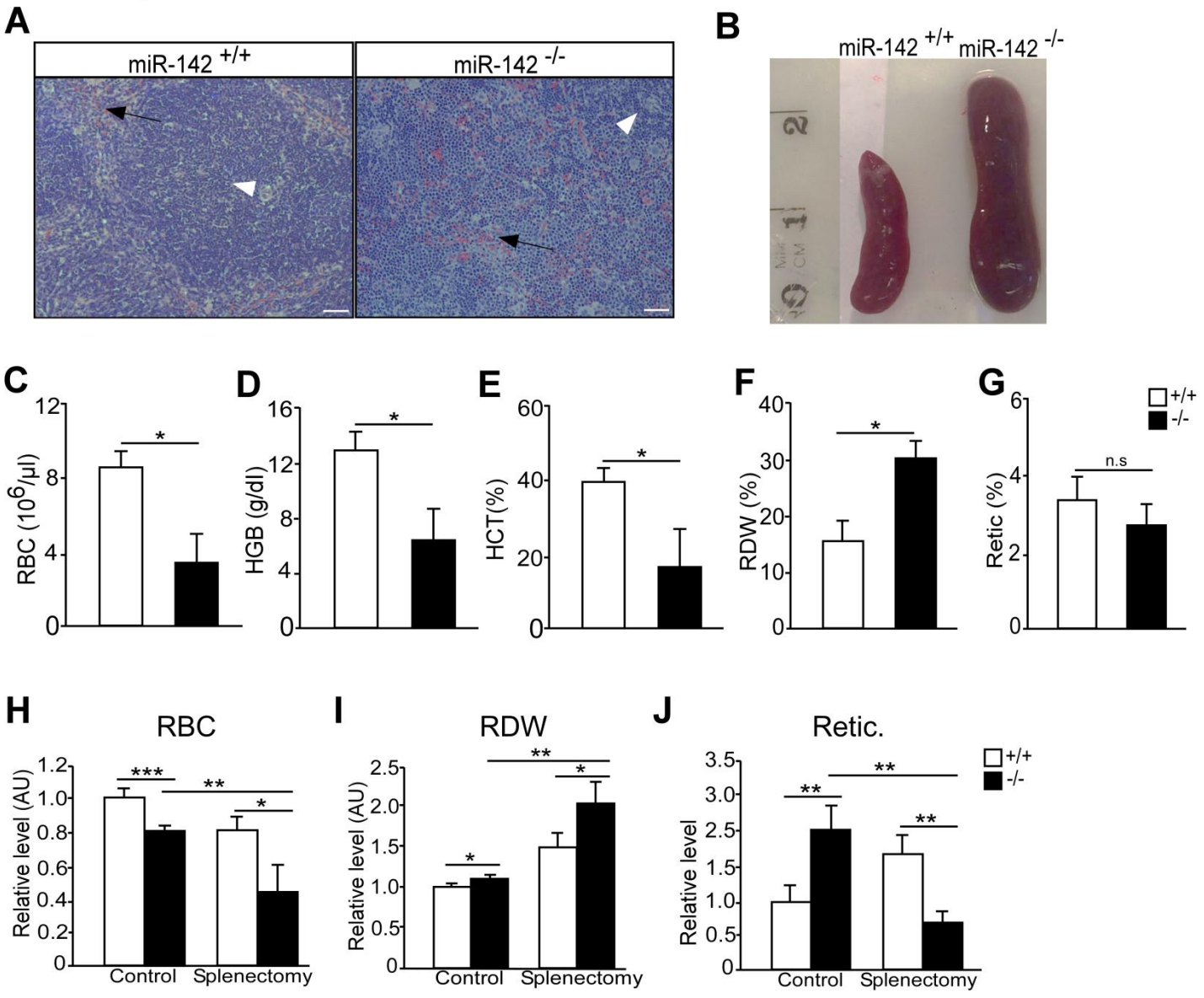


**Sup. Fig. 3: The spleen is an important synthetic organ in miR-142 -/- mice and its surgical removal results in severe anemia**. (A) Representative H&E micrograph of sectioned WT (+/+) or miR-142 deficient (–/–) spleens. Black arrows - red pulp. White arrow head - white pulp. Scale bar, 200 µm and (B) macroscopic view of spleen. Severe anemia in adult miR-142 deficient animals, one month after splenectomy, relative to controls: red blood cell numbers (RBC, C), hemoglobin (Hb, D), hematocrit (HCT, E), red cell distribution width (RDW, F) and circulating reticulocytes (Retic, G). Relative levels of complete blood count parameters, normalized to levels in un-manipulated WT control mice: (H) RBC, (I) RDW and (J) Retic (n=5 animals per group). Two tailed student t-test, Error bars, mean ±SEM, * P<0.05; ** P<0.01; *** P<0.001 ns – non significant. AU- arbitrary units.

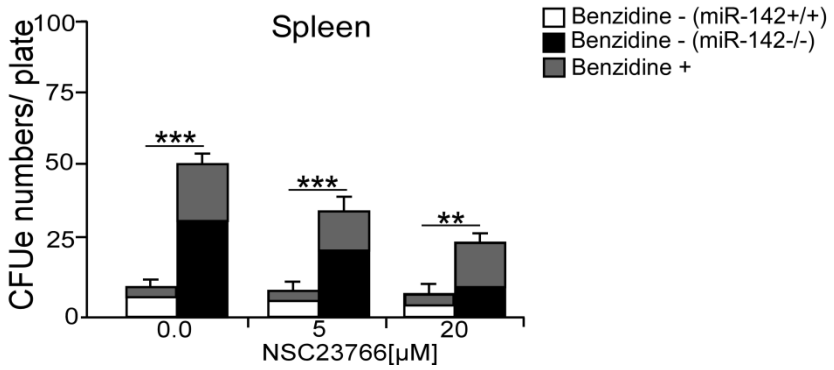


**Sup. Fig. 4: Rac1-miR-142-3p axis plays a limited role in regulating spleen erythropoiesis.** Quantification of miR-142 deficient (–/–) BFUe / CFUe from dispersed spleen, with different concentrations of Rac1 inhibitor, NSC23766. Upper bars (gray) represent the numbers of differentiating colonies, which were stained with benzidine, from total colony numbers. Two tailed student t-test, Error bars, mean ±SEM, *** $P<0.001$ ns – non significant.

Rivkin *et al*, Sup. Figure 5

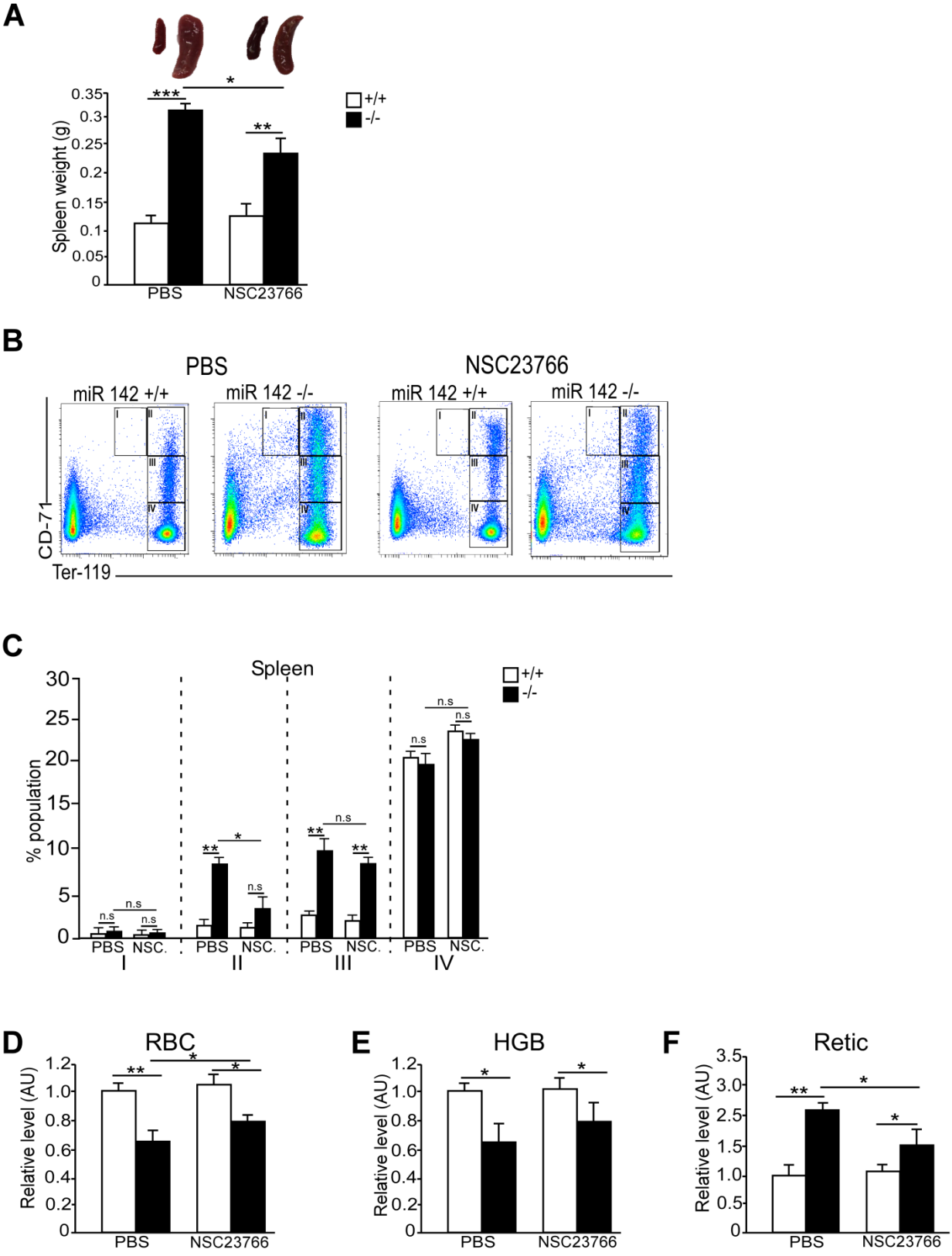

**Sup. Fig. 5: Rac1 inhibition ameliorates disease burden of miR-142 deficient animals in spleen and circulation.** WT (+/+) and miR-142 deficient (–/–) mice treated for 10 days with PBS (carrier) or with Rac1 inhibitor, NSC23766 (subcutaneous 2.5 mg /kg; n=4 per group). (A) Spleen size (in grams) and representative micrographs of an isolated organ. (B) Representative FACS profiles of erythorid populations and (C) percentile quantification. Roman numerals indicate developmentally defined subpopulations: I-Ter119$^{MED}$CD71$^{HI}$, pro-erythroblasts; II-Ter119$^{HI}$CD71$^{HI}$, basophilic erythroblasts; III- Ter119$^{HI}$CD71$^{MED}$, polychromatophilic erythroblasts; IV-Ter119$^{HI}$CD71$^{NEG}$, orthochromatophilic erythroblasts to mature erythrocytes. Bar graph of relative levels of complete blood count parameters, normalized to levels in un-manipulated WT control mice: red blood cell numbers (RBC, D), hemoglobin (HGB, E) and circulating reticulocytes (Retic, F). Two tailed student t-test, Error bars, mean ±SEM, * $P<0.05$; ** $P<0.01$; ns – non significant.

Rivkin *et al*, Sup. Figure 6

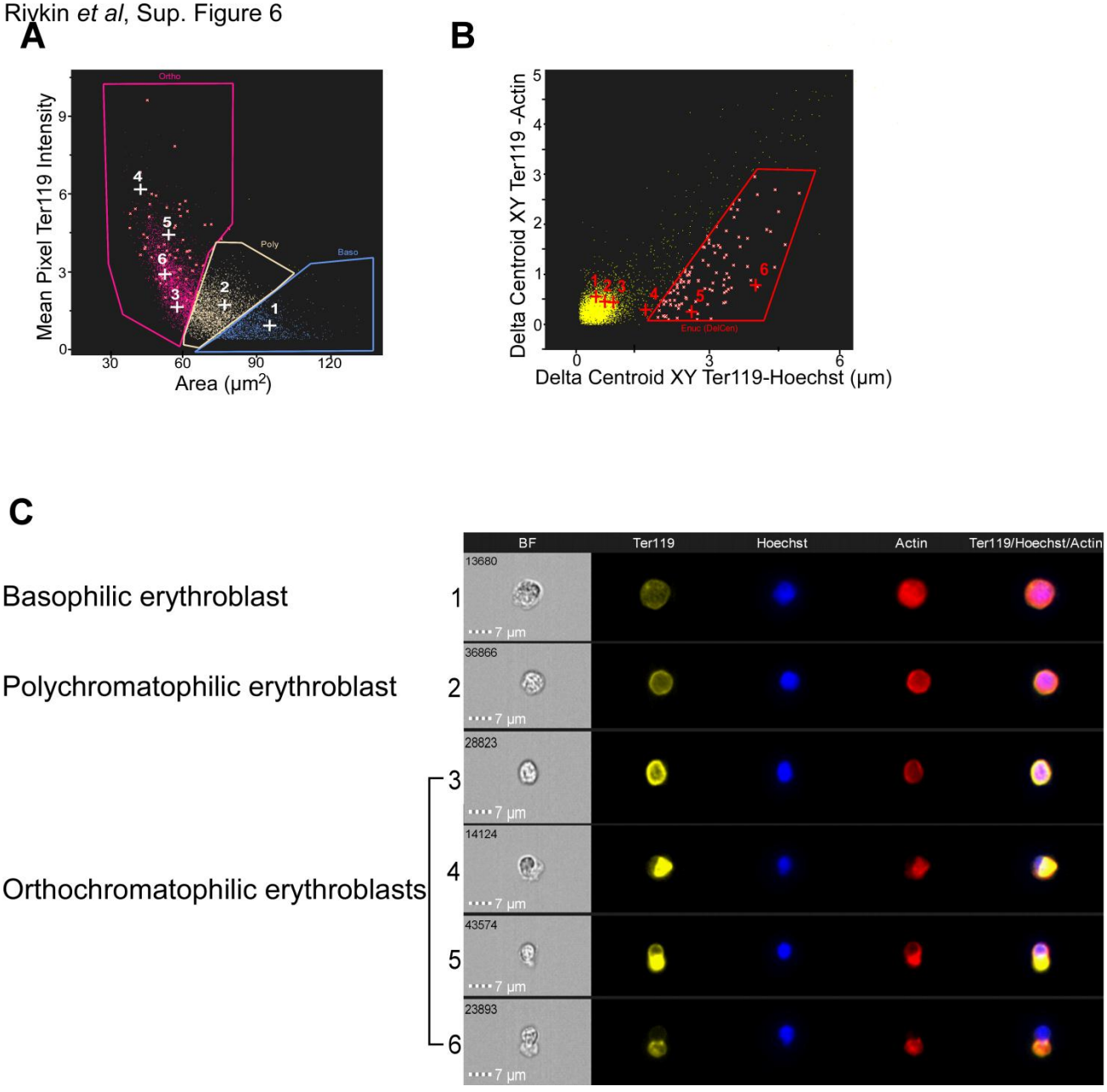


**Sup. Fig. 6: Enucleation defect in miR-142–/– erythroblasts.** (A) ImageStreamX study of enucleating erythroblasts gated on cell size (Ter119 Area) and mean Ter119 staining intensity, calling this ways basophilic (BasoE), polychromatophilic (PolyE), and orthochromatic (OrthoE) erythroblasts. (B) Erythroblasts subpopulations. "Delta centroid Ter119- Hoechst," was calculated as the distance between centers of the Ter119-signal to the center of the Hoechst signal. (D) Representative erythroid micrographs and channel separation: 647-Phalloidin (F-actin, red), Ter119-PE (yellow), and Hoechst (purple). Quantification of enucleated erythrocytes was performed on population of small Ter119$^{HI}$ cells that demonstrated highly eccentric Ter119 / Hoechst signal, as in stages 5 and 6.